

1 **Wetland eco-engineering: measuring and modeling feedbacks of oxidation**
2 **processes between plants and clay-rich material**

3 Rémon Saaltink¹, Stefan C. Dekker¹, Jasper Griffioen^{1,2}, Martin J. Wassen¹

4

5 ¹ Department of Environmental Sciences, Copernicus Institute of Sustainable
6 Development, Utrecht University, Utrecht 3508 TC, The Netherlands.

7 ² TNO Geological Survey of the Netherlands, Princetonlaan 6, 3584 CB Utrecht, The
8 Netherlands

9

10 **Corresponding author**

11 Rémon Saaltink

12 e-mail: r.m.saaltink@uu.nl

13 tel: +31 30 253 2404

14

15

16 **Abstract**

17 Interest is growing in using soft sediment as a foundation in eco-engineering
18 projects. Wetland construction in the Dutch lake Markermeer is an example: here
19 dredging some of the clay-rich lake-bed sediment and using it to construct wetland
20 will soon begin. Natural processes will be utilized during and after construction to
21 accelerate ecosystem development. Knowing that plants can eco-engineer their
22 environment via positive or negative biogeochemical plant–soil feedbacks, we
23 conducted a six-month greenhouse experiment to identify the key biogeochemical
24 processes in the mud when *Phragmites australis* is used as an eco-engineering
25 species. We applied inverse biogeochemical modeling to link observed changes in

26 pore water composition to biogeochemical processes. Two months after
27 transplantation we observed reduced plant growth and shriveling and yellowing of
28 foliage. The N:P ratios of plant tissue were low and these were affected not by
29 hampered uptake of N, but by enhanced uptake of P. Subsequent analyses revealed
30 high Fe concentrations in the leaves and roots. Sulfate concentrations rose
31 drastically in our experiment due to pyrite oxidation; as reduction of sulfate will
32 decouple Fe-P in reducing conditions, we argue that plant-induced iron toxicity
33 hampered plant growth, forming a negative feedback loop, while simultaneously
34 there was a positive feedback loop, as iron toxicity promotes P mobilization as a
35 result of reduced conditions through root death, thereby stimulating plant growth and
36 regeneration. Given these two feedback mechanisms, we propose the use of Fe-
37 tolerant species rather than species that thrive in N-limited conditions. The results
38 presented in this study demonstrate the importance of studying the biogeochemical
39 properties of the situated sediment and the feedback mechanisms between plant
40 and soil prior to finalizing the design of the eco-engineering project.

41

42 **Keywords:** Drying; Fe-P; Iron toxicity; P mobilization; PHREEQC; Pyrite

43

44

45 **1. Introduction**

46

47 Nowadays, natural processes are being used across the world to achieve fast
48 ecosystem development while at the same time providing opportunities for
49 developing hydraulic infrastructure, a concept called Building with Nature (BwN)
50 (Temmerman et al., 2013). Though mostly focused on water safety and coastal

51 protection (e.g. Borsje et al., 2011), BwN can also be applied for the management of
52 fine sediments. A relevant application could be to use soft sediments as material for
53 building freshwater wetlands. Here, vegetation can be used as an eco-engineer
54 (Jones et al., 1994), to modify the environment (Lambers et al., 2009). When fine
55 sediments are used for the construction of wetlands, however, the use of eco-
56 engineers is anticipated to pose challenges in relation to crest stability, consolidation
57 and soil formation.

58 In the Netherlands, a soft, clay-rich lake-bed sediment is causing serious turbidity
59 problems in the Markermeer (an artificial lake of 691 km²): primary productivity is
60 impeded and biodiversity in the lake is declining (Vijverberg et al., 2011; Noordhuis
61 et al., 2014). Because the lake is shallow, wind-induced waves frequently induce
62 high bed shear stress, which causes sediment to be resuspended (Vijverberg et al.,
63 2011). To improve the ecological conditions in the lake, plans are underway to
64 dredge some of the soft, clay-rich sediment and use it to construct approximately
65 10,000 ha of **wetlands**.

66 Plants produce root exudates which influence soil formation by enhancing
67 microbiological activity (Holtkamp et al., 2011), biological weathering and nutrient
68 cycling (Taylor et al., 2009; Bradford et al., 2013). An example is the ability of plant
69 roots to mobilize P by ligand exchange and dissolution of Fe-bound P (Fe-P) by
70 citrate and oxalate excretion (Gerke et al., 2000). Plant roots may also enhance
71 consolidation processes in substrate by increasing horizontal and vertical drainage
72 (O'Kelly, 2006).

73 However, both negative and positive plant–soil feedbacks exist, in which the
74 physical and chemical properties of the soil affect plant development and vice versa
75 (Ehrenfeld et al., 2005). Therefore, when looking at soil formation, it is important to

76 study the signs and strengths of these plant–soil feedback mechanisms. For
77 example, nutrient conditions co-determine the type of plant community that develops
78 (e.g. Olde Venterink, 2011), which in turn influences the nutrient conditions in the soil
79 itself (Onipchenko et al., 2001). As feedback mechanisms differ between plant
80 species (Ehrenfeld et al., 2005), it is essential to determine which eco-engineer is
81 most appropriate for accelerating ecosystem development in these sediments.

82 De Lucas Pardo (2014) found that the Markermeer mud deposits had a high water
83 content (20–60% of fresh weight) and were largely anoxic, with oxygen present only
84 in the top 2 mm. Therefore, when such mud is taken from the lake and spread out in
85 contact with the air, biogeochemical plant–soil processes related to oxidation and
86 drying of the top soil are expected to play a significant role. Two types of clay-rich
87 deposits are the intended sediment for the wetland. Their composition is the product
88 of a combination of historical and present-day factors. Prior to 1932, the year in
89 which the dam cutting off the Zuiderzee from the North Sea was completed, this was
90 a marine environment into which several rivers discharged, including a branch of the
91 river Rhine (the river IJssel). Hence, a near-shore marine deposit underlies the
92 present-day soft, clay-rich sediment. This soft, clay-rich layer is produced by
93 bioturbation and physical weathering and continuously resuspends as a result of
94 wave action (Van Kessel et al., 2008; De Lucas Pardo et al., 2013). This layer
95 accumulated after 1976, when northward sediment transport was blocked by a
96 second dam that separated Markermeer from IJsselmeer, thus allowing suspended
97 matter to resettle on top of the marine deposit. We can therefore distinguish two
98 layers: an upper disturbed mud layer prone to bioturbation and erosion, and a
99 relatively undisturbed layer below.

100 We set up an experiment to monitor the chemical composition of pore water to
101 identify the biogeochemical plant–soil feedback processes that occur when
102 oxidation, drying and modification by plants alter the biogeochemical conditions of
103 these two sediment types, thus in turn affecting vegetation development. Our study
104 has two subsidiary aims: to ascertain how *Phragmites australis* eco-engineers its
105 environment by expediting biogeochemical processes in the deposits, and to
106 simulate the geochemical differences between disturbed mud and undisturbed clay
107 deposits and relate these to the processes identified from the pore water by using
108 PHREEQC for inverse modeling. In addition, we altered the grain size of the
109 disturbed mud deposit by adding inert sand to see how grain size distribution
110 impacts pore water chemistry.

111 Changes in biogeochemical processes that are related to oxidation are expected
112 to play a major role as *P. australis* is known for its high radial oxygen loss (Brix et al.,
113 1996; Dickopp et al., 2011; Smith and Luna, 2013). Oxidation of the sediment will
114 decrease the concentration of phytotoxins typically found in waterlogged soils, such
115 as iron, and therefore will have a positive effect on plant development. This will be
116 more pronounced in undisturbed mud, which is largely anoxic, than in disturbed mud,
117 of which the top layer is already oxidized and where bioturbation modified the
118 sediment. The type of biogeochemical processes altered will depend on the intrinsic
119 properties of the different sediment types, which will be examined in this study.

120

121

122 **2. Material and Methods**

123 *2.1 Set-up*

124 A greenhouse experiment was conducted for six months at the test facility of Utrecht
125 University. A basin of 4 m² (2 x 2 m) was filled with artificial rainwater and was
126 refreshed every two weeks. At regular intervals, the chemistry of the water was
127 checked to ensure that the water composition remained stable during the
128 experiment. The artificial rainwater was made by adding 15 μmol NH₄(SO₄), 50 μmol
129 NaNO₃ and 30 μmol NaCl to osmosis water. These values reflect the average
130 rainwater composition in the Netherlands for the period 2012–2013 (LMRe, 2014).

131 The sediments used include the soft, clay-rich layer (Mud_{soft}) and the underlying,
132 consolidated, Zuiderzee deposit (Clay). In principle, both sediments have the same
133 origin and were collected in the same area. We also included a third sediment type
134 (Mud_{sand}), as it is expected that Mud_{soft} will be too soft for constructing wetlands: a
135 1:1 mixture was made by mixing mud with Dorsilit[®] crystal silica sand (c. 99% SiO₂)
136 which had been autoclaved for one hour at 120 °C prior to mixing. The sand grains of
137 this material are 0.3-0.8 mm in diameter with D50 being 0.57 mm. The Mud_{soft} and
138 Clay sediments were collected by mechanically dredging in the southern part of the
139 lake and were stored in air-tight containers at 4 °C prior to the start of the
140 experiment.

141 Plastic pots (diameter 10 cm, depth 18 cm) with a perforated base were filled to
142 within 1 cm from the top with one of the three sediment types used (t = 0). In each
143 pot, two soil moisture samplers (Rhizon Flex-5cm; Rhizosphere, Wageningen, the
144 Netherlands) were installed horizontally at depths of 1 cm and 11 cm below the
145 sediment surface (these depths are hereafter referred to as D₁ and D₁₁), its tip
146 reaching 5 cm from the pot wall. The pots were stood in rows in the basin. The water

147 level was maintained at 9 cm so that the sediment at D₁₁ remained saturated while
148 the sediment at D₁ could oxidize and dry. Each sediment type had 13 replicates.

149 Reed seedlings (*Phragmites australis*) had been grown in nutrient-poor peat and
150 when 35–40 days old (experimental time t = 22 days), a single reed seedling was
151 planted per pot in eight of the replicates, leaving five replicates unplanted. Any other
152 seedlings that germinated spontaneously in the pots were removed immediately.

153

154 2.2 Chemical analysis

155 Soil moisture at D₁ and D₁₁ was collected from the moisture samplers on days 0, 3,
156 10, 22, 36, 64, 92, 134 and 174 from five of the pots per condition. The samples from
157 the five replicates were pooled and chemically analyzed. Chloride, NH₄, NO₂, NO₃
158 and SO₄ were determined using ion chromatography (IC); Ca, Fe, K, Mn, Na, P, Si
159 and Sr were determined with Inductively Coupled Plasma Optical Emission
160 Spectrometry (ICP-OES), pH by an ion-specific electrode, and alkalinity was
161 measured by a classic titration method.

162 Sediment samples were collected for each sediment type at t = 0 and were freeze–
163 dried and stored anoxically prior to geochemical analysis. The major elements were
164 determined using ICP-OES following an aqua regia destruction. Total S content was
165 measured on an elemental CS analyzer and the mineralogical composition was
166 determined with X-ray diffraction (XRD). A sequential extraction method based on
167 Ruttenberg (1992) was applied to characterize solid P speciation. The method
168 involves five steps (Table 1), the first four of which were carried out anoxically. Loss
169 on ignition (LOI) was determined by slowly heating to 1000 °C. LOI was also used as
170 a proxy for organic matter content and total carbonates by calculating the weight loss
171 between 105–550 °C for organic matter and the weight loss between 550–1000 °C

172 for total carbonates (Howard, 1965). Cation exchange capacity (CEC) of the
173 sediments was calculated from the organic matter content and the amounts and
174 types of clay minerals present (Bauer and Velde, 2014).

175 Fifty seedlings of *P. australis* randomly chosen from the seedlings grown for the
176 experiment were used to determine the initial tissue contents of Fe, K, P, and N.
177 Their roots, shoots, and leaves were separated and air dried. The air-dried material
178 was then ground and analyzed with total reflection X-ray fluorescence (TXRF) to
179 determine tissue contents of Fe, K, and P. Nitrogen content was determined on an
180 elemental CN analyzer. At the end of the experiment (t = 174), the plants in the pots
181 were harvested and subjected to the same procedure, to determine the tissue
182 contents of Fe, K, P, and N.

183

184 *2.3 Modeling of biogeochemical processes*

185 To identify important biogeochemical processes during the incubation experiments,
186 we modeled with PHREEQC (Parkhurst and Apello, 2013). PHREEQC modeling is
187 frequently used in geochemical research focusing on issues of water quality:
188 examples include investigating mineral weathering in a mountain river (Lecomte et
189 al., 2005), deducing geochemical processes in groundwater (Belkhiri et al., 2010)
190 and investigating the interaction between two aquifers (Carucci et al., 2012). Here,
191 we applied it to identify biogeochemical plant-soil processes during the oxidation
192 and natural drying out of the soil.

193 The model approach is based on mass-balance equations of preselected mineral
194 phases (reactants). The mineral phases can either precipitate (leave the solution) or
195 dissolve (enter the solution) and these are expressed in mole transfers. As we only
196 know the dynamics in concentrations of the pore water, we applied inverse modeling

197 in which all possible combinations of the mass-balance equations are accepted
198 within a range of measured pore water concentrations $\pm 4\%$. We can simulate
199 infiltration or evaporation rates from the pore water. Since in freshwater mud
200 deposits, the dissolution or precipitation of salts (e.g. NaCl) is negligible and can be
201 ignored, the change in pore water Cl concentration was used to calculate the amount
202 of water evaporated or infiltrated.

203 To enable the model to attribute some of the chemical changes to cation-exchange
204 processes we included an assemblage of exchangers (X): CaX_2 , FeX_2 , KX , MgX_2 ,
205 NaX and NH_4X . The sum of this assemblage was defined as CEC calculated from
206 the sediment composition. CEC is important, since it can buffer some of the
207 biogeochemical processes in sediments by adsorption or desorption of cations.

208 We identified three time frames in our models: 1) oxidation and natural drying out
209 of the soil before the seedlings were transplanted into the pots ($t = 0\text{--}22$ days); 2)
210 initial stage of plant growth ($t = 22\text{--}64$ days); and 3) the stage in which roots started
211 to influence pore water chemistry ($t = 64\text{--}176$ days). These time frames were
212 identified by analysing the chemical data that was collected. When concentrations at
213 D11 in the planted condition started to deviate from the unplanted condition, this was
214 seen as a sign that plant roots started to influence pore water chemistry.

215 Inverse modeling was applied for all combinations (sediment type, plant/no plant,
216 and depth) for each time frame. For every combination, several valid simulations
217 were found, due to small differences in the amount of mole transfers attributed to the
218 mineral phases. Here we present the plausible simulation with the least amount of
219 mole transfers for each combination.

220

221 *2.4 Statistical analysis*

222 Statistical analysis was carried out using the programs R and SPSS. Differences in
223 sediment, pore water and plant tissue concentrations between sediment treatments
224 were determined using one-way ANOVA with a Tukey's honestly significant
225 difference (HSD) post hoc test. No statistics could be applied to the mineralogical
226 sediment composition (XRD analysis) due to absence of replicates.

227

228

229 **3. Results and Discussion**

230 First, the three sediment types will be compared in terms of certain geochemical and
231 mineralogical elements. Next, the composition of the pore water will be introduced
232 and will be linked to biogeochemical processes by presenting and discussing the
233 PHREEQC model simulations. Then, the plant response is presented and discussed
234 in terms of biomass and plant tissue chemistry. Lastly, the implications for eco-
235 engineering will be discussed.

236

237 *3.1 A brief comparison between sediment types*

238 Table 2 shows the geochemical composition of the disturbed Mud_{soft} and Mud_{sand}
239 and undisturbed Clay sediments used in this study. The differences between Mud_{soft}
240 and Mud_{sand} are solely attributable to the presence of inert Dorsilit[®].

241 The total sediment concentrations of Al, Fe, Mg, Mn, Na, P, and Zn were
242 significantly higher in Clay than in Mud_{soft} ($p < 0.05$). The quartz content was also
243 higher in Clay, which suggests that there were more reactive minerals in this type of
244 sediment.

245 Sequential P extraction revealed that the significant difference in total P consists of
246 a significantly lower content of Fe-P in Mud_{soft} than in Clay (279 mg/kg versus 772

247 mg/kg; $p < 0.01$); the other P pools did not differ significantly ($p = 0.11-0.94$). The
248 presence of Fe-P in the anoxic Clay sediment was unexpected, as in anoxic
249 conditions Fe prefers to bind with S to form FeS_2 . However, after exhaustion of S,
250 precipitation of Fe(II) phosphates may occur (Jilbert and Slomp, 2013). Another
251 possibility is that the reduction of crystalline Fe(III) is not complete in the anoxic
252 sediment because kinetic processes are slow (Canavan et al., 2007). This is likely
253 the case in Markermeer, given our strict anoxic procedures for storage and analysis
254 of the samples. The exchangeable (or loosely sorbed) P was low in Mud_{soft} and Clay,
255 indicating that only a small part of the total P found in the sediments was readily
256 available for uptake. The other three P-pools were fairly similar and did not differ
257 significantly between the two types of sediment ($p = 0.42$ for Ca-bound P; $p = 0.11$
258 for detrital P; and $p = 0.94$ for Organic P).

259 The mineralogical analysis (XRD) showed not only that the quartz content was
260 lower in Mud_{soft} than in Clay (37% versus 48%) but that the amounts of calcite and
261 pyrite did not differ between the two types of sediment (9% calcite and 0.6% pyrite).
262 The amount of phyllosilicates (sum of illite, smectite, kaolinite, and chlorite) was
263 higher in Mud_{soft} than in Clay: 43% versus 30%. This must also have caused the
264 CEC to be higher in Mud_{soft}, as the organic matter content did not differ much
265 between the two (7.2% in Mud_{soft} and 6.8% in Clay).

266

267 3.2 Pore water composition

268 Figure 1 presents time series for the pore water concentrations of the three
269 macronutrients N, P, and K. The initial decrease in NH_4 and increase in NO_x at a
270 depth D_1 for the planted conditions was most likely caused by nitrification as a result
271 of oxidation (Figure 1a–f). At the end of the experiment, almost all dissolved

272 inorganic nitrogen had been removed from the pore water in the pots with plants,
273 whereas in the pots without plants, the NH_4 concentrations remained substantial.
274 Furthermore, a high peak of NO_x was observed in Clay sediments at day 10 of the
275 experiment. At a depth D_{11} , no large changes were found in general for NH_4 and
276 NO_x .

277 A sharp decline in soluble P was visible at D_1 for all three sediments, probably
278 because P precipitated with Fe(III) when oxygen penetrated the top layer (Figure 1g–
279 i). However, in Clay this decline was preceded by an increase in P. After several
280 weeks, a thin moss layer started to develop on top of the Mud_{soft} sediment, which
281 probably prevented oxygen from penetrating and thereby increased the P
282 concentrations (Figure 1g). Similar developments were observed for Mud_{sand}
283 although here the moss layer developed much later. In Clay, no moss grew
284 throughout the experiment.

285 Concentrations of K were higher than concentrations of N and P and increased in
286 the first few weeks (Figure 1j–l). No difference was found between pots at D_{11} with or
287 without plants. However, K was significantly higher at D_1 in the planted pots with
288 Mud_{sand} ($p < 0.05$).

289 Although it may be important to study measured concentrations of nutrients in pore
290 water in order to understand plant functioning, deriving biogeochemical processes
291 from measured data is problematic changes in pore water can be caused by multiple
292 processes such as drying, dilution, dissolution, and precipitation. Figure 2 reveals
293 that the drying of soils at D_1 was probably an important factor, because we observed
294 an initial increase in Cl that indicated that Cl could not dissolve in the three
295 sediments used (e.g. halite dissolution). Drying will have influenced other variables
296 as well, such as sulfate (Figure 2d–f). Comparing the patterns of Cl and SO_4

297 suggests that the change in SO₄ concentrations at D₁ should be partly attributed to
298 drying out of soils and partly either to dissolution (e.g. pyrite oxidation) or to
299 precipitation (e.g. gypsum formation). This highlights the need to use geochemical
300 reaction models like PHREEQC to inversely derive biogeochemical processes from
301 measured data.

302

303 3.3 Pore water processes (PHREEQC model simulations)

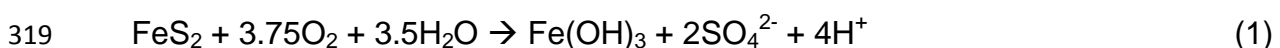
304 The main pore water processes modeled by PHREEQC are presented in Table 3.
305 For clarity, only major reactants are included in this Table. Supplementary Tables A1
306 and A2 present mole transfers for all reactants used, as well as the number of valid
307 simulations per combination found.

308

309 3.3.1 Phase 1: Oxidation and drying (t = 0–22 days)

310 As discussed in section 3.2, initial drying of soils occurred at D₁ immediately after
311 exposure to air. In the model, this is illustrated by high evaporation rates expressed
312 as H₂O loss (2300–3400 mmol l⁻¹ day⁻¹; Table 3). The model accounts for this loss
313 by adjusting the solution fractions before calculating other mole transfers.

314 Exposure to air also leads to oxidation, more so at D₁ than at D₁₁ (Table 3). The
315 increase in measured sulfate is partly explained as pyrite oxidation (109–270 μmol l⁻¹
316 day⁻¹ for D₁ and 20.1–36.2 μmol l⁻¹ day⁻¹ for D₁₁, respectively). Oxidation of pyrite
317 also produces iron oxyhydroxides and protons which in turn promotes dissolution of
318 calcite. The overall reactions are



320

321 followed by calcite dissolution



323

324 The mole transfers for pyrite and calcite presented in Table 3 indicate that not
325 enough calcite is dissolved to buffer all H^+ produced by dissolution of pyrite. Indeed,
326 a drop in pH was observed at the beginning of the experiment (not shown). However,
327 the mineralogical composition presented in Table 2 shows that the amount of calcite
328 (9%; 900 mmol) far exceeds that of pyrite (0.6%; 50 mmol). These numbers suggest
329 that even if all pyrite were to be oxidized, enough calcite is present to buffer all H^+
330 produced (200 mmol). Note that for Mud_{sand} these values are lower due to mixing
331 with Dorsilit[®].

332 Some aeration occurred at D_{11} . The O_2 fluxes ranged between 61 and 119 $\mu\text{mol l}^{-1}$
333 day^{-1} , which resulted in small amounts of pyrite being oxidized (20–36 $\mu\text{mol l}^{-1} \text{day}^{-1}$).
334 However, sulfate concentrations did not rise, as a result of subsequent precipitation
335 with Ca to form gypsum (53–73 $\mu\text{mol l}^{-1} \text{day}^{-1}$). Furthermore, the cation-exchange-
336 capacity (CEC) of the sediments buffered some processes in pore water chemistry
337 by net adsorption of cations at D_1 and net desorption at D_{11} .

338 The processes described above occurred in all three sediments, although
339 oxidation was higher in Mud_{soft} than in Mud_{sand} and Clay, probably because higher
340 evaporation rates in Mud_{soft} enhanced oxidation and affected other reactants related
341 to oxidation.

342

343 3.3.2 Phase 2: Initial stage of plant growth (t = 22–64 days)

344 While the pore water compositions did not show clear differences between unplanted
345 and planted conditions during the initial stage of plant growth, the inverse modeling
346 provided clear evidence for differences at D_1 . However, chemical differences

347 between unplanted and planted conditions for Mud_{sand} might simply be attributed to
348 concentration/dilution due to H_2O loss/gain (-996 to $380 \text{ mmol l}^{-1} \text{ day}^{-1}$).

349 Overall, more pyrite was oxidized in the planted conditions, though the rates are
350 much lower than in the first phase (0 – $64.3 \text{ } \mu\text{mol l}^{-1} \text{ day}^{-1}$). This observation provides
351 evidence that plants may enhance pyrite oxidation by radial oxygen loss (i.e. root
352 aeration). Ferric oxide production on pyrite surfaces probably impeded further
353 oxidation of pyrite, which is a common phenomenon in carbonate-buffered conditions
354 (Nicholson et al., 1990). Indeed, the total pyrite that had oxidized after 64 days (6.3
355 mmol for Mud_{soft} , 2.5 mmol for Mud_{sand} and 6.2 mmol for Clay, calculated from the
356 rates presented in Table 3) corresponds to a small fraction of total pyrite present (50
357 mmol).

358 Saturation with gypsum led to precipitation of SO_4 and Ca at D_1 . Table 3 shows
359 that with the exception of Mud_{sand} , mole transfers were lower for planted conditions;
360 the probable reason is that citric acid production by root tips retarded gypsum
361 precipitation (Prisciandaro et al., 2005). This process was not relevant at D_{11} , as
362 here aeration (and subsequent sulfate production) by plant roots was minor (in the
363 case of Clay) or absent (in the case of Mud_{soft} and Mud_{sand}).

364 The thin moss layer that started to develop after several weeks in the unplanted
365 condition on top of the Mud_{soft} sediment slowed down the aeration rate to $2.62 \text{ } \mu\text{mol}$
366 $\text{l}^{-1} \text{ day}^{-1}$ and might be the reason for the moderate increase in P, which probably
367 resulted from $\text{Fe}(\text{OH})_3$ dissolution ($0.95 \text{ } \mu\text{mol l}^{-1} \text{ day}^{-1}$) (Figure 1g, Table 3).

368

369 3.3.3 Phase 3: Root influence (t = 64–176 days)

370 Phase 3 took place in the autumn, when temperatures were lower and therefore the
371 soils did not dry out; hence there was a net gain in H₂O. The gain was less in planted
372 conditions, due to uptake of water by roots.

373 The fully grown plants continued to influence pore water chemistry at D₁, but in the
374 unplanted conditions the chemical changes were minor (Table 3). Radial oxygen loss
375 continued the oxidation processes described in the previous sections. It should be
376 noted that *P. australis* is known to have higher radial oxygen loss than other wetland
377 species (Brix et al., 1996; Dickopp et al., 2011; Smith and Luna, 2013), so the
378 aeration effect found in this study cannot be assumed to hold for other species.

379 In contrast to the previous phase, in phase 3 the influence of roots was clearly
380 visible at D₁₁ for all three sediments. All planted sediments showed increased
381 aeration and subsequent oxidation of pyrite due to radial oxygen loss, with a notable
382 difference between Mud_{soft} (lower) and Mud_{sand} (higher). This is somewhat surprising,
383 as the belowground biomass was significantly higher in Mud_{soft} (section 3.4). It
384 indicates that increasing the average grain size by adding sand enhanced aeration,
385 even when root biomass production was low.

386

387 *3.4 Plant response*

388 Above- and belowground biomass were significantly higher in Mud_{soft} and Clay than
389 in Mud_{sand} (Figure 3; $p < 0.02$). The difference between the two Mud sediments
390 cannot be explained by nutrient concentrations in pore water or light conditions in the
391 greenhouse, as these were the same for the two sediments. As biomass production
392 in Mud_{sand} was not limited by chemical or biological properties relative to Mud_{soft}, it
393 seems likely that the reason for the lower biomass production in Mud_{sand} is a
394 difference in physical properties. Voorhees et al. (1975) and Bengough and Mullins

395 (1990) showed that so-called mechanical impedance (i.e. the resistance to
396 penetration by the root tip) was higher in loamy sand than in clay, which was
397 attributed to the higher bulk density of the loamy sand. Therefore, increasing the bulk
398 density of Mud_{soft} by mixing with sand increased the mechanical impedance and this
399 might explain the lower biomass production we observed in Mud_{sand}.

400 *P. australis* invested more in its root system than in its shoots and leaves for all
401 sediments (Figure 3; $p < 0.01$). More investment in roots implies a limitation of N, P,
402 and/or S (Ericsson, 1995; Shipley and Meziane, 2002). Figures 1a–i and 2d–f show
403 that the N and P concentrations were indeed low in the planted conditions but that
404 SO₄ was high, which rules out S limitation. During the experiment, we had observed
405 reduced plant growth and shriveling and yellowing of foliage 2 months after
406 transplantation, which might have been caused by nutrient limitation.

407 Figure 4 shows the N, P, and K contents as well as the N:P ratio for the roots of *P.*
408 *australis* at the beginning and end of the experiment for the three sediment types.
409 The N, P, and K contents in the roots increased in time, while the N:P ratio clearly
410 decreased. The reduction in N:P ratio from 11 to 2–3 suggests N was the limiting
411 nutrient as an N:P ratio of < 14 in plant tissue is indicative of N limitation
412 (Koerselman and Meuleman, 1996). However, root N and P concentrations of *P.*
413 *australis* should typically range between 0.64–1.04% for N and 0.06–0.13% for P
414 (Wang et al., 2015). Figure 4 shows that the root N and P concentrations were above
415 these values, and that P was particularly high: by a factor of 5 to 10 (N: 1.14–1.63%
416 and P: 0.52–0.62%). Hence the concentrations of these nutrients in the roots do not
417 indicate that nutrient limitation is a likely cause of the reduced plant growth and
418 shriveling and yellowing of foliage.

419 We hypothesize that co-precipitation of P with Fe on roots enhanced the
420 concentrations of P in the plant roots (Snowden and Wheeler, 1995; Jørgenson et
421 al., 2012). Snowden and Wheeler (1995) showed that this so-called iron plaque
422 formation enhances uptake of Fe and P. This may cause iron toxicity and is probably
423 responsible for the elevated P concentrations in tissue, and for the stunted growth
424 and leaf decay we observed in the experiment. Note that the plant roots of *P.*
425 *australis* initiate this process by oxidizing their environment and thereby enabling
426 ferrous iron to oxidize into P-bearing ferric iron, which precipitates on roots.

427 The Fe concentration in the leaves and in the roots supports the “Fe-P co-
428 precipitation hypothesis”: we measured an approximately 20-fold increase by
429 comparison with the initial concentration in the seedlings (Figure 5). Furthermore,
430 ferric oxide, a product of pyrite oxidation, precipitates on root surfaces (Jørgenson et
431 al., 2012), and hence pyrite oxidation in sediments is directly linked to iron toxicity in
432 plants.

433 Further evidence to support our hypothesis is provided by the results of the
434 sequential phosphorus extraction conducted on the sediments: it revealed that the
435 dominant P pool in the sediments is the Fe-P fraction (Table 2). P co-precipitates
436 with Fe on roots if it is bound to ferric oxides.

437

438 *3.5. Implications for eco-engineering*

439 Our results strongly point in the direction of iron toxicity as a major bottleneck
440 prohibiting healthy development of *P. australis*. Since the candidate material for the
441 construction of the Markermeer wetland has high contents of Fe and Fe-P, we
442 recommend using Fe-tolerant plant species as test species in the new wetland,
443 rather than species optimized for growing in N-limited conditions.

444 Concomitantly with iron toxicity, a high Fe-P content in soil will trigger P
445 mobilization if that soil is rewetted after having dried out and contains high amounts
446 of SO₄ (Smolders and Roelofs, 1993; Lucassen et al., 2005). In some cases, this can
447 result in elevated levels of sulfide, thereby promoting S toxicity in plants (Lamers et
448 al., 1998; Van der Welle et al., 2007).

449 Figure 6 summarizes the important feedbacks and processes we expect play an
450 important role in the clay-rich sediments. Following the feedback loops between
451 plant and soil, we see a negative feedback loop that arises because plant roots
452 induce aeration, which promotes iron toxicity that decreases plant growth and results
453 in plant death. Also, we see a positive feedback loop, as iron toxicity induces
454 reduction processes as a result of root death, which leads to P mobilization and
455 hence enhances plant growth and regeneration. Negative feedback loops diminish or
456 buffer changes, whereas a positive feedback loop amplifies changes. So, a negative
457 feedback loop normally stabilizes the system, in our case via the toxic effect of iron
458 oxides on plants, but plant growth may increase due to the positive feedback loop via
459 P mobilization. The relative strengths of these two feedback loops and the sensitivity
460 of species to Fe toxicity determine the ultimate effect on vegetation development in
461 wetlands built from these sediments.

462 As drying–rewetting cycles are likely to occur in these future wetlands and since
463 the Fe-P concentrations in the situated sediment are high, these feedbacks might be
464 an important factor influencing soil formation and ecosystem development. We
465 therefore recommend studying the ultimate effects of the use of this material on
466 ecosystem development by testing with various plant species and drying–rewetting
467 cycles.

468 Not all environmental factors that potentially interfere with the processes and
469 feedbacks described in this study could be taken into account with this experimental
470 design (e.g. wave action, wind). Therefore, we recommend to carry out experiments
471 on the wetlands themselves once the crest has stabilized sufficiently.

472

473

474 **4. Conclusions**

475 The results of this study show that plants expedite biogeochemical processes by
476 oxidizing and modifying their environment, which in turn affects the growth conditions
477 of the plants. In the mud deposits from Markermeer, the key processes influencing
478 pore water chemistry are pyrite oxidation and associated calcite dissolution. The
479 former is especially likely to be important as it is linked to iron toxicity and P
480 mobilization and thus has the potential to initiate two feedback mechanisms between
481 plant and soil. We found strong indications for a negative feedback loop, where
482 plant-induced iron toxicity is hampering plant growth, and a positive feedback loop,
483 where iron toxicity promotes P mobilization, enhancing plant growth. The strength of
484 these feedbacks and the balance between them will play an important role in
485 regulating eco-engineering conditions for plants.

486 We found conclusive evidence that the low N:P ratio found in plant tissue was not
487 caused by N limitation, as the ratio suggests, but probably results from enhanced P
488 uptake as a result of co-precipitation with Fe on roots.

489 The magnitudes of the feedback mechanisms are expected to differ between the
490 sediments used. The soft clay-rich layer has less Fe-P than the underlying clay layer
491 and therefore P mobilization is expected to be less in mud. However, when the mud
492 is mixed with sand, the enhanced aeration due to the change in grain-size

493 composition results in higher oxidation rates, increasing the impact of the positive
494 feedback mechanisms involving P mobilization and iron toxicity.

495 To study the effects of iron toxicity and P mobilization in greater detail, we
496 recommend further testing with different plant species and drying–rewetting cycles.
497 This is important because we expect these mechanisms to influence soil formation
498 and ecosystem development in the created wetlands.

499

500 **Acknowledgements**

501 This study was supported with funding from Netherlands Organization for Scientific
502 Research (NWO), project no. 850.13.032 and the companies Boskalis and Van
503 Oord. We would also like to thank Botanical Garden Utrecht for their help, support
504 and advice during the greenhouse experiment. Joy Burrough advised on the English.
505 Last, we would like to thank Ingrid Bauer and an anonymous referee for helpful
506 comments on the manuscript.

507 **References**

- 508 Bauer, A., Velde, B.D.: Soils: Retention and Movement of Elements at the Interface,
509 in: Geochemistry at the Earth's Surface: Movement of Chemical Elements, Springer-
510 Verlag Berlin Heidelberg, New York, 2014.
- 511
- 512 Belkhir, L., Boudoukha, A., Mouni, L., Baouz, T.: Application of multivariate statistical
513 methods and inverse geochemical modeling for characterization of groundwater — A
514 case study: Ain Azel plain (Algeria), *Geoderma*, 159, 390-398, 2010.
- 515
- 516 Bengough, A.G., Mullins, C.E.: Mechanical impedance to root growth: a review of
517 experimental techniques and root growth responses, *Journal of Soils Science*, 41,
518 341-358, 1990.
- 519
- 520 Borsje, B.W., Van Wesenbeeck, B.K., Dekker, F., Paalvast, P., Bouma, T.J., Van
521 Katwijk, M., De Vries, M.B.: How ecological engineering can serve in coastal
522 protection, *Ecological Engineering*, 37, 113-122, 2011.
- 523
- 524 Bradford, M.A., Keiser, A.D., Davies, C.A., Mersmann, C.A., Strickland, M.S.:
525 Empirical evidence that soil carbon formation from plant inputs is positively related to
526 microbial growth, *Biogeochemistry*, 113, 271-281, 2013.
- 527
- 528 Brix, H., Borrell, B.K., Schierup, H.H.: Gas fluxes achieved by in situ convective flow
529 in *Phragmites australis*, *Aquatic Botany*, 54, 151-163, 1996.
- 530
- 531 Canavan, R.W., Van Cappellen, P., Zwolsman J.J.G., Van den Berg, G.A., Slomp,
532 C.A.: Geochemistry of trace metals in a fresh water sediment: Field results and
533 diagenetic modeling, *Science of the Total Environment*, 381, 263–279, 2007.
- 534
- 535 Carucci, V., Petitta, M., Aravena, R.: Interaction between shallow and deep aquifers
536 in the Tivoli Plain (Central Italy) enhanced by groundwater extraction: A multi-isotope
537 approach and geochemical modeling, *Applied Geochemistry*, 27, 266-280, 2012.
- 538
- 539 De Lucas Pardo, M.A., Bakker, M., Van Kessel, T., Cozzoli, F., Winterwerp, J.C.:
540 Erodibility of soft freshwater sediments in Markermeer: the role of bioturbation by
541 meiobenthic fauna, *Ocean Dynamics*, 63, 1137-1150, 2013.
- 542
- 543 De Lucas Pardo, M.A.: Effect of biota on fine sediment transport processes. A study
544 of lake Markermeer, Ph.D thesis, Delft University, the Netherlands, 211 pp., 2014.
- 545
- 546 Dickopp, J., Kazda, M., Cízková, H.: Differences in rhizome aeration of *Phragmites*
547 *australis* in a constructed wetland, *Ecological Engineering*, 37, 1647-1653, 2011.
- 548

549 Ehrenfeld, J.G., Ravit, B., Elgersma, K.: Feedback in the plant-soil system, Annual
550 Review of Environment and Resources, 30, 75-115, 2005.
551

552 Ericsson, T.: Growth and shoot:root ratio of seedlings in relation to nutrient
553 availability, Plant and Soil, 168, 205-214, 1995.
554

555 Gerke, J., Beissner, L., Römer W.: The quantitative effect of chemical phosphate
556 mobilization by carboxylate anions on P uptake by a single root. I. The basic concept
557 and determination of soil parameters, Journal of Plant Nutrition and Soil Science,
558 163, 207-212, 2000.
559

560 Holtkamp, R., Van der Wal, A., Kardol, P., Van Putten, W.H., De Ruiter, P.C.,
561 Dekker, S.C.: Modelling C and N mineralisation in soil food webs during secondary
562 succession on ex-arable land, Soil Biology and Biochemistry, 43, 251-260, 2011.
563

564 Howard, P.J.A.: The Carbon-Organic Matter Factor in Various Soil Types, Oikos, 15,
565 229-236, 1965.
566

567 Jilbert, T., Slomp C.P.: Iron and manganese shuttles control the formation of
568 authigenic phosphorus minerals in the euxinic basins of the Baltic Sea, Geochimica
569 et Cosmochimica Acta, 107, 155–169, 2013.
570

571 Jones, C.G., Lawton, J.H., Shachak, M.: Organisms as Ecosystem Engineers, Oikos,
572 69, 373-386, 1994.
573

574 Jørgenson, K.D., Lee, P.F., Kanavillil, N.: Ecological relationships of wild rice,
575 *Zizania* spp. 11. Electron microscopy study of iron plaques on the roots of northern
576 wild rice (*Zizania palustris*), Botany, 91, 189–201, 2012.
577

578 Koerselman, W., Meuleman, A.F.M.: The vegetation N:P ratio: a new tool to detect
579 the nature of nutrient limitation, Journal of Applied Ecology, 33, 1441-1450, 1996.
580

581 Lambers, H., Mougél, C., Jaillard, B., Hinsinger P.: Plant-microbe-soil interactions in
582 the rhizosphere: an evolutionary perspective, Plant and Soil, 321, 83-115, 2009.
583

584 Lamers, L.P.M., Tomassen, H.B.M., Roelofs J.G.M.: Sulfate-Induced Eutrophication
585 and Phytotoxicity in Freshwater Wetlands, Environmental Science and Technology,
586 32, 199-205, 1998.
587

588 Lecomte, K.L., Pasquini, A.I., Depetris, P.J.: Mineral weathering in a Semiarid
589 Mountain River: Its assessment through PHREEQC inverse modeling, Aquatic
590 Geochemistry, 11, 173-194, 2005.
591

592 LMRe (Landelijk Meetnet Regenwater): <http://www.lml.rivm.nl/gevalideerd/>, last
593 access: 17 November 2014, 2014.
594

595 Lucassen, E.C.H.E.T., Smolders, A.J.P., Lamers, L.P.M., Roelofs, J.G.M.: Water
596 table fluctuations and groundwater supply are important in preventing phosphate-
597 eutrophication in sulphate-rich fens: Consequences for wetland restoration, *Plant
598 and Soil*, 269, 109-115, 2005.
599

600 Nicholson, R.V., Gillham, R.W., Reardon E.J.: Pyrite oxidation in carbonate-buffered
601 solution: 2. Rate control by oxide coatings, *Geochimica et Cosmochimica Acta*, 54,
602 395-402, 1990.
603

604 Noordhuis, R., Groot, S., Dionisio Pires, M., Maarse M.: Wetenschappelijk
605 eindadvies ANT-IJsselmeergebied. Vijf jaar studie naar kansen voor het ecosysteem
606 van het IJsselmeer, Markermeer en IJmeer met het oog op de Natura-2000 doelen,
607 Open File Rep. 1207767-000, 98 pp., 2014.
608

609 Olde Venterink, H.: Does phosphorus limitation promote species-rich plant
610 communities?, *Plant and Soil*, 345, 1-9, 2011.
611

612 O'Kelly, B.C.: Compression and consolidation anisotropy of some soft soils,
613 *Geotechnical and Geological Engineering*, 24, 1715-1728, 2006.
614

615 Onipchenko, V.G., Makarov, M.I., Van der Maarel, E.: Influence of alpine plants on
616 soil nutrient concentrations in a monoculture experiment, *Folia Geobotanica*, 36,
617 225-241, 2001.
618

619 Parkhurst, D.L., Appelo, C.A.J.: Description of input and examples for PHREEQC
620 version 3-A computer program for speciation, batch-reaction, one-dimensional
621 transport, and inverse geochemical calculations, U.S. Geological Survey, Denver,
622 497 pp., 2013.
623

624 Prisciandaro, M., Santucci, A., Lancia, A., Musmarra, D.: Role of citric acid in
625 delaying gypsum precipitation, *The Canadian journal of Chemical Engineering*, 83,
626 586-592, 2005.
627

628 Ruttenberg, K.C.: Development of a sequential extraction method for different forms
629 of phosphorus in marine sediments, *Limnology Oceanography*, 37, 1460-1482, 1992.
630

631 Shipley, B., Meziane D.: The balanced-growth hypothesis and the allometry of leaf
632 and root biomass allocation, *Functional Ecology*, 16, 326-331, 2002.
633

634 Smith, K.E., Luna, T.O.: Radial Oxygen Loss in Wetland Plants: Potential Impacts on
635 Remediation of Contaminated Sediments, *Journal of Environmental Engineering*,
636 139, 496-501, 2013.

637

638 Smolders, A., Roelofs J.G.M.: Sulphate-mediated iron limitation and eutrophication in
639 aquatic ecosystems, *Aquatic Botany*, 46, 247-253, 1993.

640

641 Snowden, R.E.D., Wheeler, B.D.: Chemical changes in selected wetland plant
642 species with increasing Fe supply, with specific reference to root precipitates and Fe
643 tolerance, *New Phytologist*, 131, 503-520, 1995.

644

645 Taylor, L.L., Leake, J.R., Quirk, J., Hardy, K., Banwart, S.A., Beerling, D.J.:
646 Biological weathering and the long-term carbon cycle: integrating mycorrhizal
647 evolution and function into the current paradigm, *Geobiology*, 7, 171-191, 2009.

648

649 Temmerman, S., Meire, P., Bouma, T.J., Herman, P.M.J., Ysebaert, T., De Vriend,
650 H.K.: Ecosystem-based coastal defence in the face of global change, *Nature*, 504,
651 79-83, 2013.

652

653 Van der Welle, M.E.W., Smolders, A.J.P., Op den Camp, H.J.P., Roelofs, J.G.M.,
654 Lamers, L.P.M.: Biogeochemical interactions between iron and sulphate in
655 freshwater wetlands and their implications for interspecific competition between
656 aquatic macrophytes, *Freshwater Biology*, 52, 434-447, 2007.

657

658 Van Hees, P.A.W., Jones, D.L., Finlay, R., Godbold, D.L., Lundström U.S.: The
659 carbon we do not see—the impact of low molecular weight compounds on carbon
660 dynamics and respiration in forest soils: a review, *Soil Biology and Biochemistry*, 37,
661 1-13, 2005.

662

663 Van Kessel, T., De Boer, G., Boderie P.: Calibration suspended sediment model
664 Markermeer, Open File Rep. 4612, 107 pp., 2008.

665

666 Vijverberg, T., Winterwerp, J.C., Aarninkhof, S.G.J., Drost, H.: Fine sediment
667 dynamics in a shallow lake and implication for design of hydraulic works, *Ocean*
668 *Dynamics*, 61, 187-202, 2011.

669

670 Voorhees, W.B., Farrel, D.A., Larson, W.E.: Soil strength and aeration effects on root
671 elongation, *Soil Science Society of America Journal*, 39, 948-953, 1975.

672

673 Wang, W.Q., Sardans, J., Wang, C., Zeng, C.S., Tong, C., Asensio, D., Penuelas, J.:
674 Ecological stoichiometry of C, N, and P of invasive *Phragmites australis* and native
675 *Cyperus malaccensis* species in the Minjiang River tidal estuarine wetlands of China,
676 *Plant Ecology*, 216, 809-822, 2015.

677 **Table 1.** List of steps used in the extraction procedure of phosphorus (based on
 678 Ruttenberg, 1992).

Step	Extractant	Separated P fraction
I	1M MgCl ₂ , 30 min	Exchangeable or loosely sorbed P
II	A Citrate-dithionite-bicarbonate (CDB), 8 h	Easily reducible or reactive ferric Fe- P
	B 1M MgCl ₂ , 30 min	
III	A Na acetate buffer (pH 4), 6 h	Amorphous apatite and carbonate P
	B 1M MgCl ₂ , 30 min	
IV	1M HCl, 24 h	Crystalline apatite and other inorganic P
V	Ash at 550 °C, 2h; 1M HCl, 24 h	Organic P

679 **Table 2.** Geochemical and mineralogical composition of the sediment types used in
 680 this study. Significant differences between Mud_{soft} and Clay are indicated by * (p <
 681 0.05).

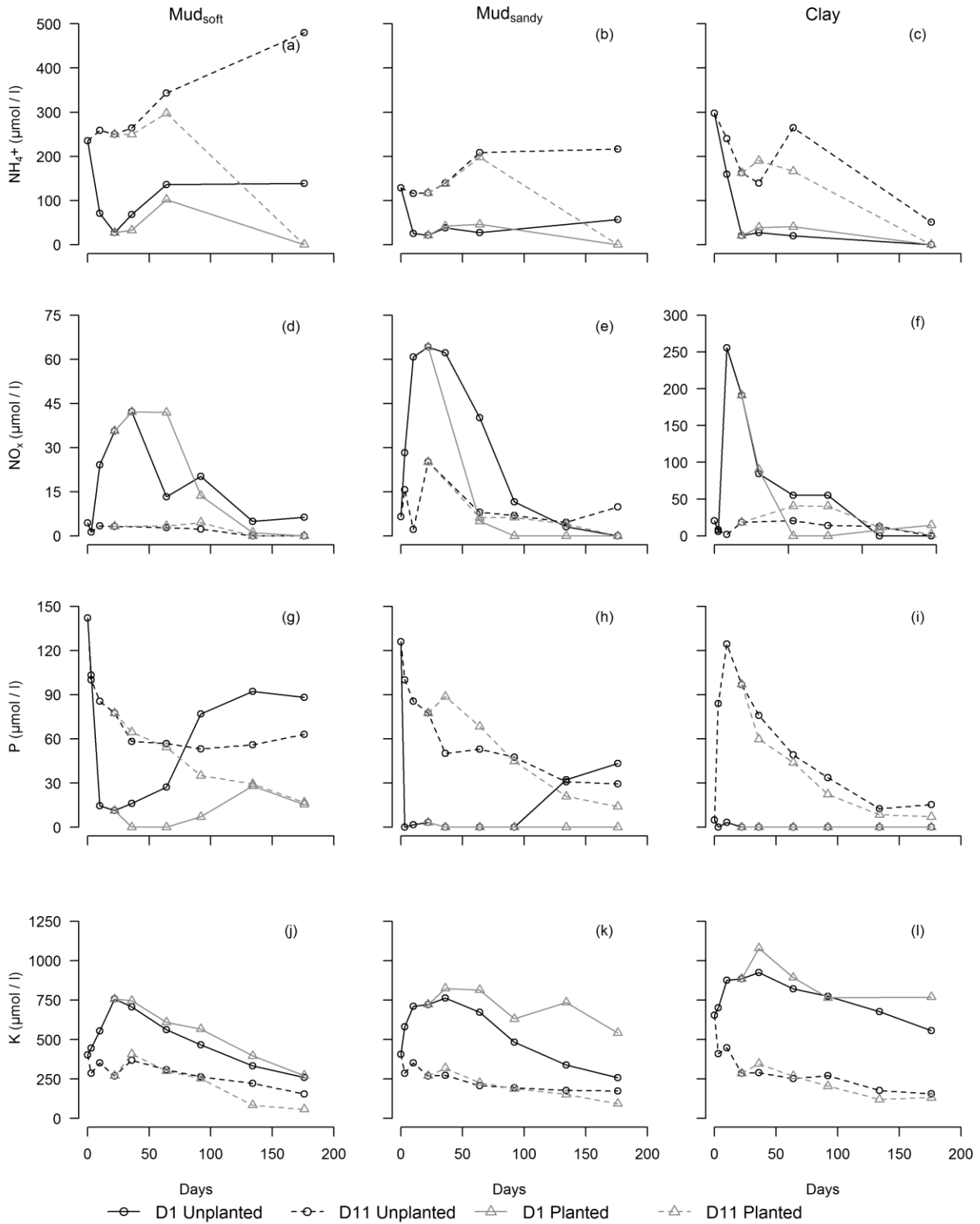
	Unit	n per type	Clay Mean	SD	Mud _{soft} Mean	SD	Mud _{sand} Mean	SD
<i>Aqua regia / CS</i>								
Al*	mg/kg	15	21989	4512	16593	3130	6394	2439
Ca	mg/kg	15	48031	3032	45635	6020	18877	3572
Fe*	mg/kg	15	27766	3764	20745	2987	7804	2281
K	mg/kg	15	5371	1262	4102	641	1723	742
Mg*	mg/kg	15	8041	1017	6636	906	2531	558
Mn*	mg/kg	15	710	166	577	160	238	62
Na*	mg/kg	15	992	379	526	158	219	64
P*	mg/kg	15	1186	217	649	169	259	56
S	mg/kg	15	5727	710	5586	698	3001	846
Sr	mg/kg	15	148	21	135	26	62	14
Ti	mg/kg	15	312	74	312	77	125	44
Zn*	mg/kg	15	159	58	110	29	43	18
<i>Seq. P extraction</i>								
Exchangeable P	mg/kg	15	14.3	6.81	11.9	3.50	5.9	1.79
Fe- bound P*	mg/kg	15	772	263	279	61.7	94.5	29.0
Ca-bound P	mg/kg	15	146	43.3	121	30.9	36.8	13.1
Detrital P	mg/kg	15	147	16.5	169	14.1	51.5	10.9
Organic P	mg/kg	15	99.6	20.0	117	25.1	47.7	8.38
<i>XRD</i>								
Quartz	%	1	48		37		n.a.	
Calcite	%	1	9		9		n.a.	
Pyrite	%	1	0.6		0.6		n.a.	
Illite	%	1	15		21		n.a.	
Smectite	%	1	11		14		n.a.	
Kaolinite	%	1	3		5		n.a.	
Chlorite	%	1	2		3		n.a.	
<i>Other</i>								
Organic matter	%	5	6.7	0.6	7.2	0.6	2.8	0.4
CEC (calculated)	meq/100g		30.0		37.2		12.4	

682

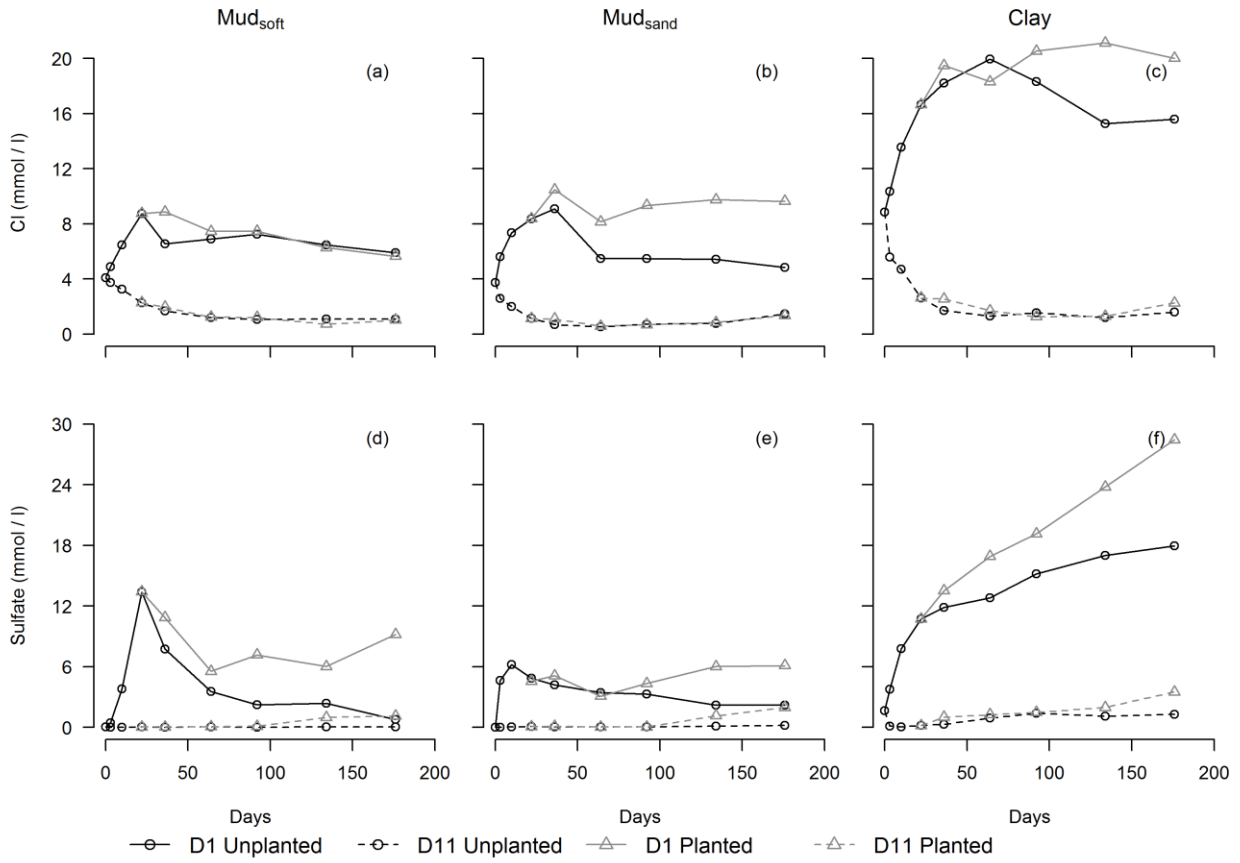
683 **Table 3.** Main pore water processes expressed in mole transfers ($\mu\text{mol l}^{-1} \text{ day}^{-1}$) as modeled by PHREEQC with pore water data
 684 retrieved at 1 cm and 11 cm below sediment surface (D_1 and D_{11} respectively). Positive values indicate dissolution, negative values
 685 indicate precipitation. Cation exchange capacity (CEC) is the sum of Ca, Fe, K, Mg, Na, and NH_4 .

Phase	Condition	Calcite		Gypsum		$\text{Fe}(\text{OH})_3$		Pyrite		ΣCEC		$\text{H}_2\text{O} (\times 10^3)$		O_2	
		D_1	D_{11}	D_1	D_{11}	D_1	D_{11}	D_1	D_{11}	D_1	D_{11}	D_1	D_{11}	D_1	D_{11}
1. Oxidation t=0-22 days	Mud_{soft} No plant	267	111	0.00	-72.5	-277	0.00	270	36.2	-31.3	20.2	-3364	0.00	1009	119
	Mud_{sand} No plant	0.00	59.6	0.00	-40.7	-116	0.00	109	21.7	-4.99	7.92	-2591	0.00	432	69.5
	Clay No plant	120	55.2	0.00	-53.4	-160	0.00	159	20.1	-91.4	14.0	-2364	0.00	659	61.9
2. Initial root development t=22-64 days	Mud_{soft} No plant	27.1	0.00	-236	0.00	0.95	-0.24	0.00	0.00	-23.1	1.43	0.00	0.00	2.62	0.00
	Mud_{soft} Plant	48.8	19.8	-208	-3.81	-10.0	-6.19	9.76	0.00	-7.63	1.43	0.00	0.00	45.5	0.00
	Mud_{sand} No plant	39.3	71.7	0.00	0.00	0.00	-41.2	0.21	0.00	1.90	1.46	380	0.00	0.00	0.00
	Mud_{sand} Plant	7.10	83.8	-83.4	0.00	0.00	-51.2	3.58	0.00	5.40	3.40	-996	0.00	0.00	0.00
	Clay No plant	0.00	27.1	-32.1	0.00	-21.4	-25.0	21.2	0.00	0.01	-0.23	-286	0.00	41.9	0.00
	Clay Plant	36.9	16.2	0.00	0.00	-14.3	0.00	64.3	11.9	28.4	4.53	-6.67	0.00	186	40.5
3. Root influence t=64-176 days	Mud_{soft} No plant	0.00	-3.21	-19.2	0.00	-1.34	-0.80	0.00	0.00	-1.07	-1.43	56.3	0.00	0.00	0.00
	Mud_{soft} Plant	25.8	0.00	0.00	0.00	-4.20	0.00	23.8	4.11	7.88	-4.65	49.1	0.00	83.6	13.6
	Mud_{sand} No plant	8.13	0.00	-7.59	0.00	-10.6	-1.34	0.00	0.00	-1.78	1.42	74.1	0.00	0.00	0.00
	Mud_{sand} Plant	0.00	0.00	-14.8	0.00	-13.3	-23.2	13.8	7.95	0.12	-10.6	-357	-652	44.7	32.6
	Clay No plant	0.00	11.5	0.00	0.00	0.00	-13.8	33.3	0.00	23.9	0.36	134	0.00	113	0.00
	Clay Plant	115	18.7	0.00	0.00	-58.5	-8.48	58.3	8.57	45.4	-5.73	0.00	-98.2	215	28.4

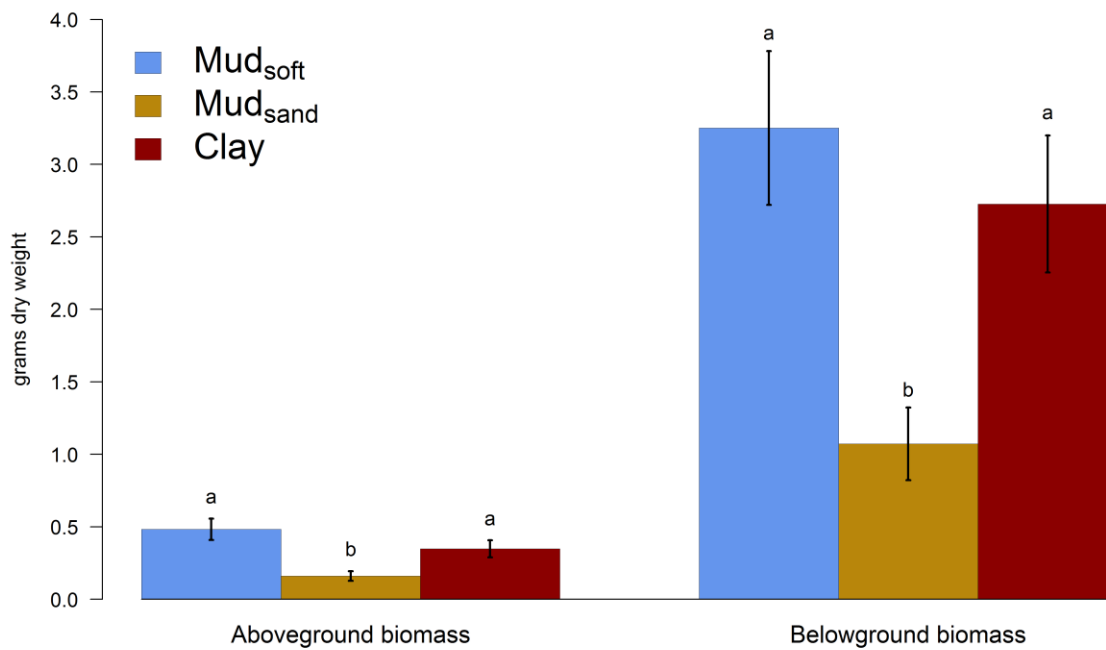
686



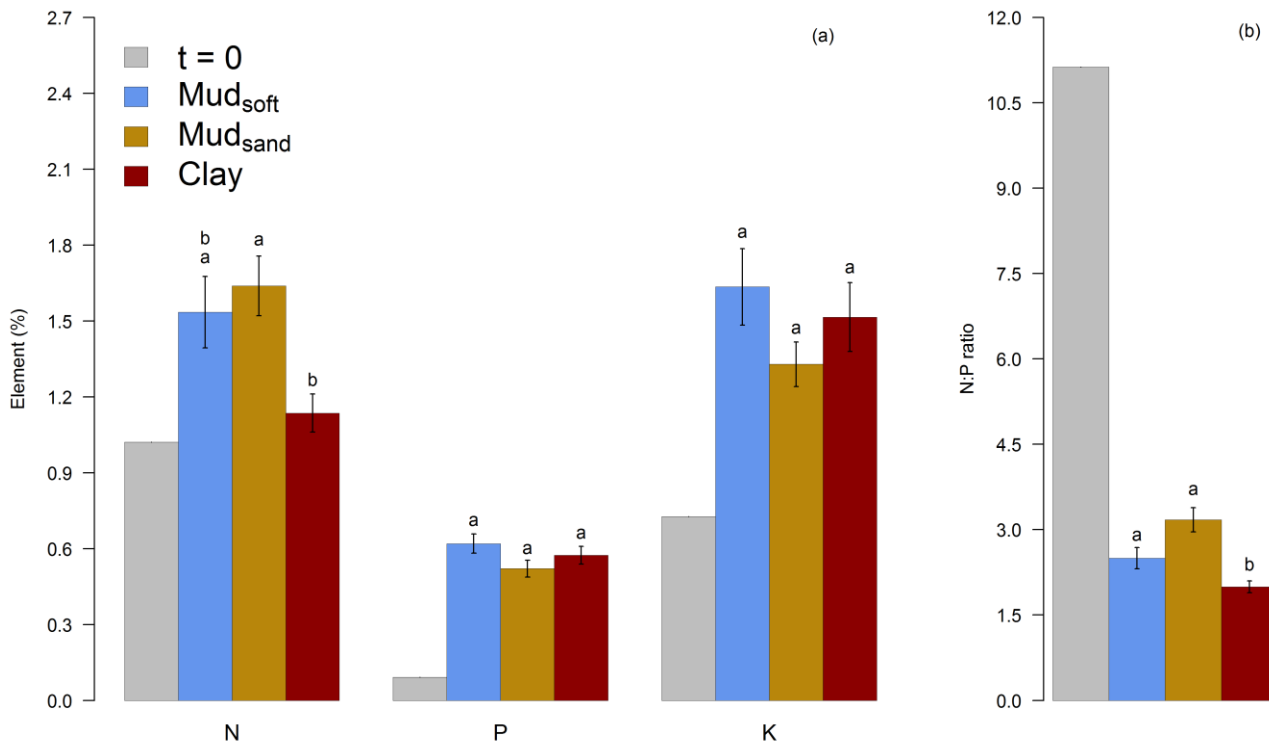
687 **Figure 1.** Time series of NH₄ (a–c), NO_x (d–f), P (g–i) and K (j–l) concentrations.
 688 Each column represents one sediment type: Mud_{soft} (a, d, g, j), Mud_{sandy} (b, e, h, k),
 689 and Clay (c, f, i, l). The variable and the scale of the x-axis are the same for each
 690 row, except for the scale in f.



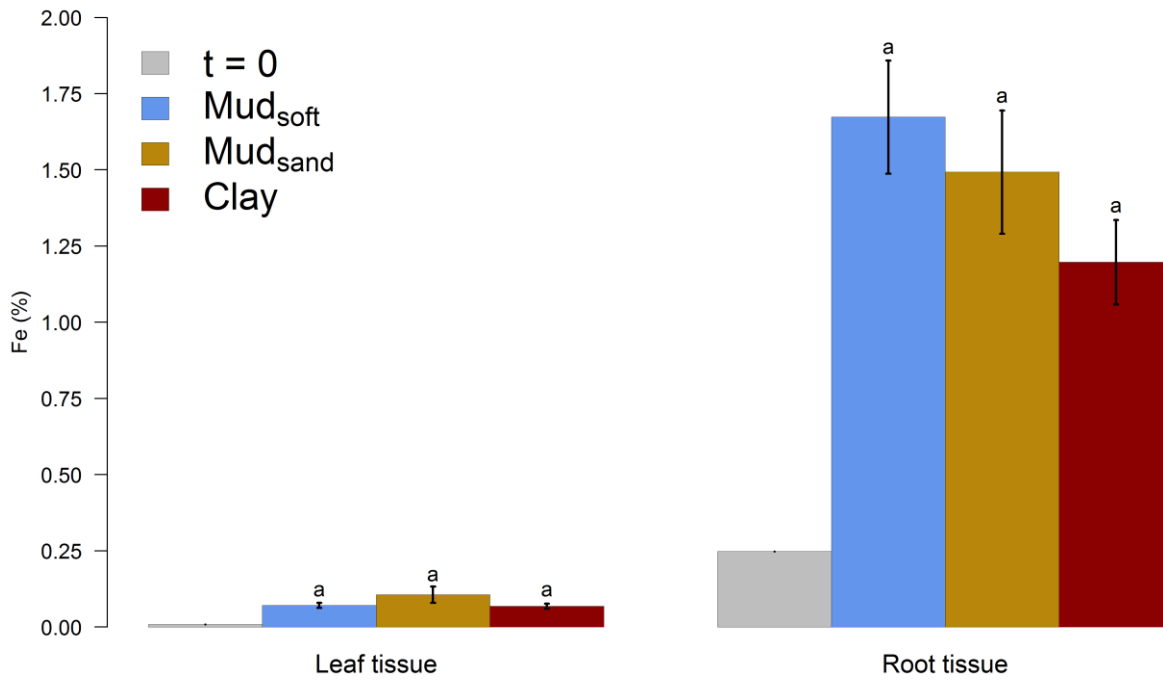
691 **Figure 2.** Time series of Cl (a–c) and sulfate (d–f) concentrations. Each column
 692 represents one sediment type: Mud_{soft} (a, d), Mud_{sand} (b, e), and Clay (c, f). The
 693 variable and the scale of the x-axis are the same for each row.



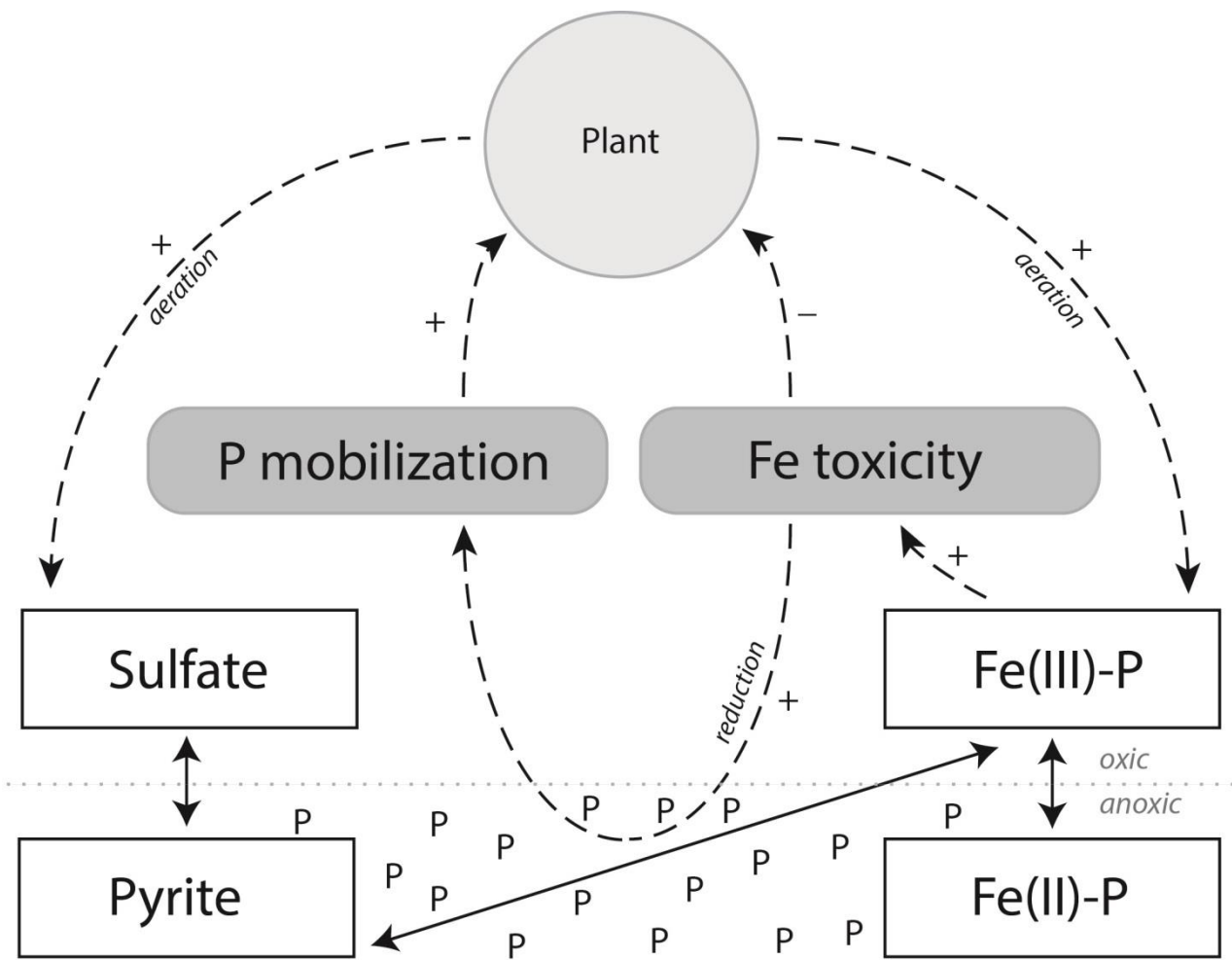
694 **Figure 3.** Above- and belowground biomass in grams dry weight, with error bars (n =
 695 5). Significant differences between sediment types are indicated by different letters,
 696 and non-significant differences are indicated by a similar letter.



697 **Figure 4.** N, P, and K concentration in root tissue (t = 176) in % of dry weight (a) as
 698 well as the N:P ratio (b) with error bars when n = 5. Significant differences between
 699 sediment types are indicated by different letters, and non-significant differences are
 700 indicated by a similar letter.



701 **Figure 5.** Fe concentration (% of dry weight) in leaf and root tissue with error bars
 702 when n = 5. Significant differences between sediment types are indicated by different
 703 letters, and non-significant differences are indicated by a similar letter.



704 **Figure 6.** Most important biogeochemical processes and feedbacks identified in this
 705 study. + indicates positive feedback, - indicates negative feedback.

706 **Appendix**

707

708 **Table A1.** Pore water processes expressed in mole transfers ($\mu\text{mol l}^{-1} \text{ day}^{-1}$) as modeled by PHREEQC with pore water data
 709 retrieved at 1 cm below sediment surface. Positive values indicate dissolution, negative values indicate precipitation.

Reactant	Composition	Phase 1. Oxidation (t=0-22)			Phase 2. Initial root development (t=22-64)						Phase 3. Root influence (t=64-176)					
		No plant Mud _{soft}	No plant Mud _{sand}	No plant Clay	No plant Mud _{soft}	Plant	No plant Mud _{sand}	Plant	No plant Clay	Plant	No plant Mud _{soft}	Plant	No plant Mud _{sand}	Plant	No plant Clay	Plant
Calcite	CaCO ₃	267	0.00	120	27.1	48.8	39.3	7.1	0.00	36.9	0.00	25.8	8.13	0.00	0.00	115
Gypsum	CaSO ₄ :2H ₂ O	0.00	0.00	0.00	-236	-208	0.00	-83.4	-32.1	0.00	-19.2	0.00	-7.59	-14.8	0.00	0.00
Hydroxyapatite	Ca ₅ (PO ₄) ₃ (OH)	-5.00	-3.64	0.00	0.24	0.00	-0.02	-0.04	0.00	0.00	0.18	0.00	0.09	0.00	0.00	0.00
Chalcedony	SiO ₂	-19.1	-15.5	-18.2	0.95	0.71	1.91	-3.37	-1.67	-2.14	0.71	0.00	0.54	1.43	0.00	-0.36
Fe(OH) ₃ (a)	Fe(OH) ₃	-277	-116	-160	0.95	-10.0	0.00	0.00	-21.4	-14.3	-1.34	-4.20	-10.6	-13.3	0.00	-58.5
Pyrite	FeS ₂	270	109	159	0.00	9.76	0.21	3.58	21.2	64.3	0.00	23.8	0.00	13.8	33.3	58.3
Rhodochrosite	MnCO ₃	-11.8	-11.4	-2.27	2.86	1.19	1.23	0.34	-0.24	-0.24	-0.63	-0.89	0.09	0.18	0.00	0.00
CEC	CaX ₂	0.00	20.9	55.5	63.1	41.9	-9.11	0.00	0.00	0.00	2.50	0.00	-9.73	0.00	-9.64	-85.4
	FeX ₂	0.00	0.00	0.00	0.00	0.00	-0.19	-4.11	0.00	-50.2	1.61	-19.8	11.7	0.00	-33.3	0.00
	KX	-8.64	-5.00	-17.7	-4.76	0.00	3.78	-8.30	-6.19	0.00	-2.14	-2.14	-2.77	-7.68	0.00	0.00
	MgX ₂	31.4	-16.8	36.8	-39.8	-30.5	7.42	-1.35	0.00	21.7	-3.04	12.0	0.00	0.00	19.1	39.8
	NaX	-20.9	0.00	-166	-46.4	-25.7	0.00	25.1	25.2	77.6	0.00	19.7	0.00	12.0	49.4	92.9
	NH ₄ X	-33.2	-4.09	0.00	4.76	6.67	0.00	-5.94	-19.0	-20.7	0.00	-1.88	-0.98	-4.20	-1.70	-1.88
H ₂ O (g)	H ₂ O x 10 ³	-3364	-2591	-2364	0.00	0.00	380	-996	-286	-6.67	56.3	49.1	74.1	-357	134	0.00
O ₂ (g)	O ₂	1009	432	659	2.62	45.5	0.00	0.00	41.9	186	0.00	83.6	0.00	44.7	113	215
CO ₂ (g)	CO ₂	-827	-532	-650	35.2	0.00	39.7	0.00	-55.5	-84.8	0.00	-33.1	0.00	44.6	-31.7	-115
No. models found		2	2	2	3	4	2	2	5	2	6	2	1	2	2	1

710

711 **Table A2.** Pore water processes expressed in mole transfers ($\mu\text{mol l}^{-1} \text{ day}^{-1}$) as modeled by PHREEQC with pore water data

712 retrieved at 11 cm below sediment surface. Positive values indicate dissolution, negative values indicate precipitation.

Reactant	Composition	Phase 1. Oxidation (t=0-22)			Phase 2. Initial root development (t=22-64)						Phase 3. Root influence (t=64-176)					
		No plant Mud _{soft}	No plant Mud _{sand}	No plant Clay	No plant Mud _{soft}	Plant	No plant Mud _{sand}	Plant	No plant Clay	Plant	No plant Mud _{soft}	Plant	No plant Mud _{sand}	Plant	No plant Clay	Plant
Calcite	CaCO ₃	111	59.6	55.2	0.00	19.8	71.7	83.8	27.1	16.2	-3.21	0.00	0.00	0.00	11.5	18.7
Gypsum	CaSO ₄ :2H ₂ O	-72.5	-40.7	-53.4	0.00	-3.81	0.00	0.00	0.00	0.00	0.00	0.00	0.00	0.00	0.00	0.00
Hydroxyapatite	Ca ₅ (PO ₄) ₃ (OH)	0.00	0.51	1.45	-0.24	0.00	0.00	0.00	0.00	0.00	0.00	-0.09	0.00	-0.45	0.00	-0.18
Chalcedony	SiO ₂	4.44	5.32	6.74	1.90	3.33	3.10	3.81	1.67	0.95	-0.18	-1.07	-0.27	-3.48	0.00	-1.07
Fe(OH) ₃ (a)	Fe(OH) ₃	0.00	0.00	0.00	-0.24	-6.19	-41.2	-51.2	-25.0	0.00	-0.80	0.00	-1.34	-23.2	-13.8	-8.48
Pyrite	FeS ₂	36.2	21.7	20.1	0.00	0.00	0.00	0.00	0.00	11.9	0.00	4.11	0.00	7.95	0.00	8.57
Rhodochrosite	MnCO ₃	0.00	1.18	0.31	0.00	0.48	1.19	0.95	0.00	0.24	0.00	0.00	0.00	-0.71	0.18	0.09
CEC	CaX ₂	0.00	0.00	0.00	-1.43	-5.95	-50.7	-63.3	-7.86	0.00	1.70	8.39	0.00	0.00	-3.75	0.00
	FeX ₂	-35.5	-20.9	-19.0	0.00	0.00	42.4	51.7	0.00	-11.9	1.07	-3.66	-0.54	15.2	4.29	0.00
	KX	7.00	5.87	3.76	0.00	0.00	2.62	2.86	-5.95	1.67	-0.89	-1.79	0.00	-3.84	0.00	-1.70
	MgX ₂	15.4	13.0	4.87	0.00	4.76	7.14	8.57	8.10	7.38	-1.25	0.00	0.00	-4.11	2.59	5.71
	NaX	25.2	9.95	24.4	0.00	0.00	0.00	5.24	0.00	6.43	-4.29	-4.20	1.96	-12.4	0.00	-5.54
	NH ₄ X	8.12	0.00	0.00	2.86	2.62	0.00	-1.67	5.48	0.95	2.23	-3.39	0.00	-5.80	-2.77	-4.20
H ₂ O (g)	H ₂ O x 10 ³	0.00	0.00	0.00	0.00	0.00	0.00	0.00	0.00	0.00	0.00	0.00	0.00	-652	0.00	-98.2
O ₂ (g)	O ₂	119	69.5	61.9	0.00	0.00	0.00	0.00	0.00	40.5	0.00	13.6	0.00	32.6	0.00	28.4
CO ₂ (g)	CO ₂	156	0.00	43.0	0.00	0.00	0.00	0.00	0.00	14.5	0.00	0.00	0.00	-67.3	0.00	-13.7
No. models found		2	2	1	4	4	2	2	3	2	1	4	2	4	2	1

713

714